

Available online at www.sciencedirect.com

jmr&t
Journal of Materials Research and Technology
journal homepage: www.elsevier.com/locate/jmrt



Original Article

Flexibility properties of pressure-sensitive adhesive with different pattern of crosslinking density for electronic displays



Ji-Soo Kim ^a, Hyun-Joong Kim ^{a,b,*}, Yoong-Do Kim ^{c,**}

^a Laboratory of Adhesion and Bio-Composites, Department of Agriculture, Forestry and Bioresources, Seoul National University, Seoul, 08826, Republic of Korea

^b Research Institute of Agriculture and Life Sciences, College of Agriculture & Life Sciences, Seoul National University, Seoul, 08826, Republic of Korea

^c Samsung Display Co., Ltd., Cheonan, 31086, Republic of Korea

ARTICLE INFO

Article history:

Received 2 March 2021

Accepted 30 August 2021

Available online 2 September 2021

Keywords:

Optically clear pressure-sensitive adhesive

UV curing Pattern

Flexible display

Stress relaxation property

Strain recovery property

ABSTRACT

Displays in electronic devices visualize digital information, which is essential for humans to ultimately understand and use the Internet of Things (IoT) technology. Along with the evolution of several electrical components for flexible displays, developing flexible pressure-sensitive adhesives (PSA) is also important. In this study, a pattern of crosslinking density was applied to a PSA during the ultraviolet (UV) curing process to secure adhesion, transparency, stress relaxation, and supplement the strain recovery performance. We measured the modulus of each pattern region by atomic force microscopy (AFM) and confirmed whether the UV pattern PSA was prepared through the implementation of differential crosslinking density. Additionally, we measured dynamic mechanical analysis (DMA) strain recovery test, rheometer, peel strength, probe tack, and transmittance to confirm the effect of the given crosslinking density pattern on the overall physical properties of PSA.

© 2021 The Authors. Published by Elsevier B.V. This is an open access article under the CC BY-NC-ND license (<http://creativecommons.org/licenses/by-nc-nd/4.0/>).

1. Introduction

In modern electronic devices, the display, as a standard human–machine interface, is a core component [1,2]. It connects user feedback and machine data by visually conveying the world of bits to humans. Therefore, the display will enable humans to understand and use the Internet of Things (IoT)

technology, which will lead to the fourth industrial revolution and rapid development [3–6]. The display is also being studied to realise a new form factor that is wearable [7–9] and flexible (foldable, stretchable, and rollable) for human use. Despite technological advances in flexible and stretchable electronic components such as flexible electrodes and organic light emitting diodes (OLEDs), perfect assembly remains a challenge. With the development of display technology, pressure-

* Corresponding author.

** Corresponding author.

E-mail addresses: hjokim@snu.ac.kr (H.-J. Kim), colour.kim@samsung.com (Y.-D. Kim).

<https://doi.org/10.1016/j.jmrt.2021.08.145>

2238-7854/© 2021 The Authors. Published by Elsevier B.V. This is an open access article under the CC BY-NC-ND license (<http://creativecommons.org/licenses/by-nc-nd/4.0/>).

sensitive adhesives (PSA) have been commonly used to assemble display components [10] because of their high viscoelasticity [11]. In addition, their gap filling ability minimises the discrepancy in the refractive index, thereby clarifying the displayed image [12]. A PSA adheres to the substrate under low pressure, and can be peeled off without residue [13]. It is also easily introduced into the display assembly process because it does not require post-treatments such as solvent drying and heat treatment after bonding under pressure [14,15]. Among the PSA composition, acrylic, silicone, and urethane compositions are typical [16]. In particular, acrylic PSAs are transparent by themselves, do not require an additional tackifier [17], and are mainly used as optically clear pressure-sensitive adhesive (OCA) materials in display assembly. However, existing acrylic PSAs are rigid and irreversible when stretched [18], developing flexible and transparent PSAs remains critical for the successful implementation of flexible displays. The physical properties of acrylic PSAs applied to flexible displays have been actively studied [11,19,20]. As a result, the trade-off relationship between the peel strength and strain recovery performance has been discussed.

This study was conducted to improve flexibility while maintaining adhesive performance and transparency by applying a curing density pattern to the PSA sheet by selectively irradiating ultraviolet (UV) light by using a photomask with a pattern in the UV curing system [21]. PSA's flexibility was analyzed in terms of strain recovery and stress relaxation because the recovery performance prevents plastic deformation, and the stress relaxation performance prevents delamination due to internal cracks. Preceding researches show the relation of dynamic mechanical analysis (DMA) storage modulus and recovery/relaxation properties [22]. Generally, the recovery property increases as the storage modulus increases, whereas the stress relaxation property is the opposite. The recovery property and relaxation property of the PSA are in an inverse relationship. The UV patterned OCA we designed contains high cured regions and low cured regions according to the photomask pattern, and each cured region reveals different property respectively. Additionally, the region having a high curing density formed an overall storage modulus to the PSA and maintained resistance to external stress around the crosslinking site, thereby exhibiting excellent recovery property. The low cured region had a synergistic effect of reducing the deformation rate of the high cured region and preventing plastic deformation by exhibiting a buffering effect, as the polymer chain easily slides and stretches as it deforms from the outside.

After the UV pattern curing was applied to the acrylic PSA pre-polymer, the modulus of each pattern was measured to identify its formation. Further, the relationship between the

curing density of each pattern and the modulus of the entire sample was identified. In addition, stress recovery, stress relaxation, peel strength, and probe tack properties were analysed to determine the physical properties of the resulting cured PSA, which exhibit differential modulus properties. Transmittance was measured to examine its applicability to the OCA. In this study, curing density pattern was introduced in the UV curing system, resulting in improved stress relaxation performance while maintaining stress relaxation performance, which has not been done yet. This can be a crucial advancement in the field of flexible OCA material processing.

2. Materials and methods

2.1. Preparation of UV-patterned acrylic PSA film

The acrylate oligomer (2100M, Winnerschem Corp., Republic of Korea) was used as base adhesive resin (Mw: 40653, PDI: 2.31, Viscosity: 51 cP at 20 °C, 200 rpm, Refractive index: 1.4412 at 20 °C). The glass transition temperature of uncured acrylate oligomer measured by differential scanning calorimetry (DSC Q200, TA Instruments, USA) is -10 °C. Polyethylene glycol 200 diacrylate (Miramer M282, Miwon Specialty Chemical Co., Ltd., Republic of Korea) was used as the crosslinking agent. Ethyl phenyl (2,4,6-trimethylbenzoyl) phosphinate (Omnirad 2100, Shinyoung Rad, Chem., Ltd.) was used as the photoinitiator. A UV 365 nm LED light source was used for the curing process.

An acrylic oligomer blended with 1 phr of the photoinitiator and crosslinking agent was coated between silicon-treated polyethylene terephthalate release films (PET, SKC Co., Ltd., Republic of Korea) by an applicator. The thickness of the coated oligomer blend was 60 µm. The coated oligomer blend was irradiated by a UV LED lamp (area curing system, 365 nm, 7 mW/cm²) for primary curing. The distance between lamp and coating was 4 cm. The UV energy ranged from 0 to 4 J for each sample (Table 1). The detailed curing process is shown in Fig. 1 (a). After the primary curing was completed, photo mask film is put on the primary cured PSA sheet and perform secondary curing by irradiating UV LED light on it. The photo mask film is placed directly on top of the release film. Fig. 1b shows a schematic diagram and the size of the curing degree of the UV-pattern cured PSA. There is a variation in patterns 1–9 depending on the difference in curing density between isolated region and line region of the pattern. The surface area of each isolated and line region is composed of a 1:1 ratio. The number of radicals generated from the photoinitiator depends on the irradiated UV energy. Therefore, the number of radical reactions with the C=C double bond and the crosslinking densities of the irradiated sections

Table 1 – UV curing conditions of UV patterned PSA samples.

Pattern No.	1	2	3	4	5	6	7	8	9
UV Irradiated Energy of Line Region (J)	0	0.5	1	1.5	2	2.5	3	3.5	4
UV Irradiated Energy of Island Region (J)	4	3.5	3	2.5	2	1.5	1	0.5	0
Irradiation Energy Difference between Patterns (J)	-4	-3	-2	-1	0	1	2	3	4

vary. As a result, a UV-patterned PSA sheet composed of two sections with different crosslinking densities is manufactured.

2.2. Viscoelastic properties

The Young's modulus (E , modulus of elasticity) of each cured section of the pattern was measured using atomic force microscopy (AFM, NX-10, Park Systems, Republic of Korea) in a pinpoint mode with pressing 0.8 V. The contact depth of the material with the probe was 10–50 nm, and the force was less than 10 nN. The AFM tip PPP-NCSTR (NANOSENSORS™, guaranteed tip radius of curvature <10 nm, tip height 10–15 μm) was used to measure each cured region. The PSA coated onto the PET sheet was first cut into 5×5 mm samples. The PSA film was then peeled off, and fixed to an AFM sample holder. The force–distance curve was measured at 10 points. The Young's modulus was calculated using the Oliver and Pharr model [23,24].

Viscoelastic properties of the whole PSA sample containing both low and high cured region, including storage modulus (G , modulus of shearing elasticity) and glass transition temperature were measured using a rheometer (MCR302, Anton Paar,

Austria). The oscillatory temperature sweep experiments of the samples were conducted at an angular frequency of 10 rad/s. The strain was 1%, and the preloading force was 1 N. The probe diameter was 8 mm. The measuring PSA sample diameter was 8 mm, containing both high cured and low cured region.

2.3. Strain recovery and stress relaxation

DMA (Q800, TA Instruments, USA) in the tension film mode was used to evaluate the strain recovery and stress relaxation properties of the PSA sheet. The release film covering cured PSA sheet was peeled off and the cured PSA sheet was attached between the polycarbonate substrate (IS-Optics Co., Ltd) cut into 3×0.6 cm², with the adhesion area of 2×0.6 cm². The thickness of the polycarbonate substrate was 1 mm. A constant shear strain (50%) was applied for 10 min, and then the force was decreased to zero for 5 min. The PSA experienced the shear strain between the polycarbonate substrates because the strain was applied in the tensile direction. The strain recovery (%) and stress relaxation (%) were calculated using the Eq. (1) from our previous work [19].

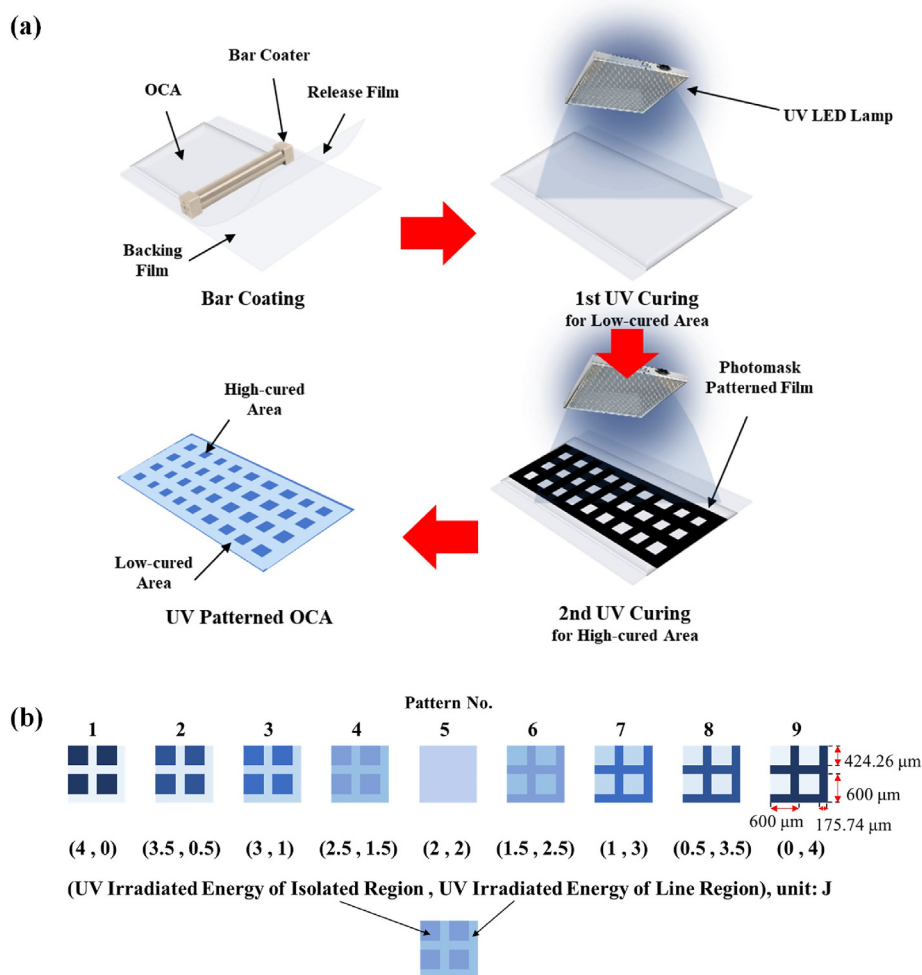


Fig. 1 – (a) Process of manufacturing the UV patterned PSA sample. (b) Schematic diagram of the curing degree of UV patterned PSA containing quantitative size of the pattern repeating unit.

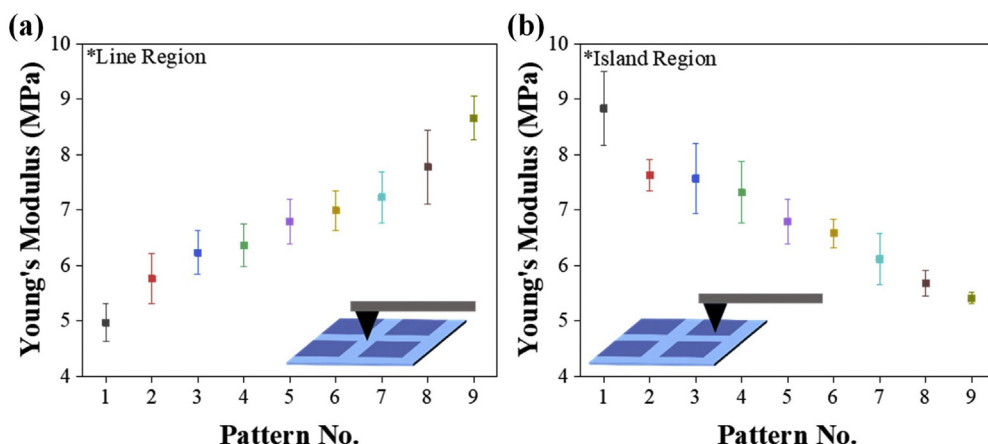


Fig. 2 – Young's modulus data of (a) line and (b) isolated region of the UV pattern cured PSA samples.

Strain recovery (%) = $(S_0 - S_t) / S_0 \times 100$ (1)

Stress relaxation (%) = $(F_i - F_f) / F_i \times 100$ (2)

2.4. Adhesion properties

Based on ASTM D3330, the bonded specimens were prepared as 25-mm-wide samples to measure the 180° peel strength using a texture analyser (TA-XT2i, Micro Stable Systems, UK). The specimens were left to stand at 20 °C 55% RH for 24 h prior to testing. A peeling test crosshead speed of 300 mm/min was

employed at 20 °C. The force (N) was recorded for three different runs, and the average force was recorded as N/ 25 mm. The measurement was performed 5 times to calculate the average value and standard deviation.

The probe tack was measured using a texture analyser (TA-XT2i, Micro Stable Systems, UK) with a 5-mm diameter stainless steel cylinder probe at 20 °C. In the first step, the approaching speed of the probe was 0.5 mm/s. In the second step, the probe was in contact with the surface of the OCAs for 1 s at a constant pressure of 100 g/cm², and the debonding speed was 0.5 mm/s. A probe tack was used to measure the

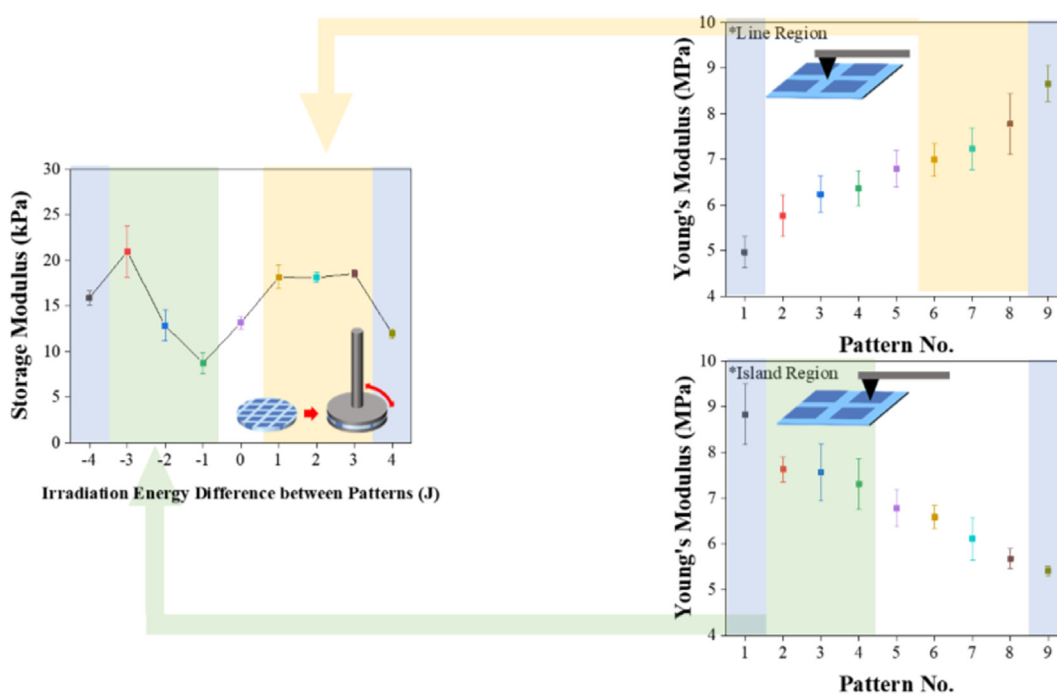


Fig. 3 – Storage modulus data measured by rheometer of the UV pattern cured PSA samples (25 °C, angular frequency of 10 rad/s). The graphic displays relationship and property influence mechanism between Young's modulus of each patterned region and storage modulus of the entire sample.

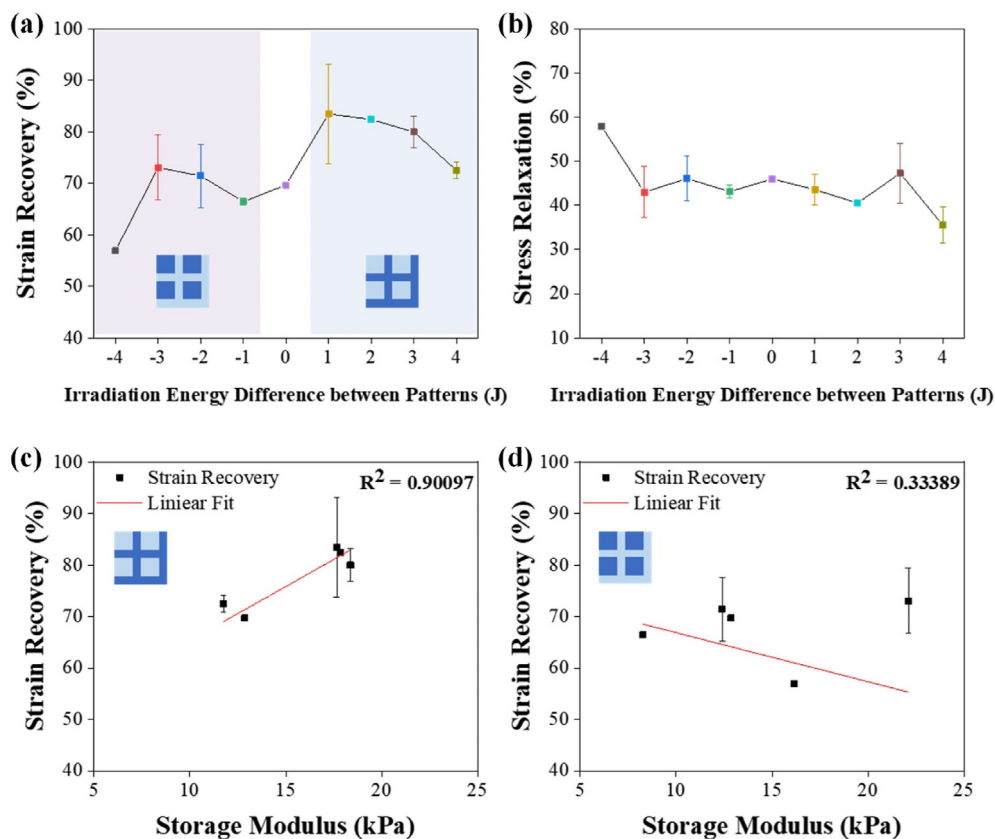


Fig. 4 – (a) Strain recovery property, and (b) stress relaxation property of the UV pattern cured PSA samples. The relationship between the storage modulus and strain recovery, with the trend line calculated by the least squares method, (c) pattern 5 and 4–9 composed of a highly cured connected region (d) pattern 5 and 1–4 composed of a highly cured isolated region.

maximum debonding force. The measurement was performed 7 times to calculate the average value and standard deviation.

2.5. Transmittance

The transmittance of the UV-cured acrylic OCAs was examined using UV–visible spectroscopy (UV-2550, Shimadzu, Japan), with empty air as the reference. The transmittance was determined to be in the visible range of 400–800 nm.

3. Results and discussion

3.1. Identification of the UV pattern formation

The AFM measurement has clear significance in confirming the formation of the curing pattern by showing that there is a difference in Young's modulus for each high and low cured region according to the curing pattern. Each cured region of the samples showed different Young's modulus values like shown in Fig. 2. In the pattern 1 (Fig. 1b) sample, the Young's modulus value of the isolated region was 8.6 MPa, whereas that of the line region was 4.9 MPa. By measuring with AFM, the isolated and line regions of each pattern-cured sample showed different Young's modulus values, confirming the

formation of UV curing patterns. As pattern number increased, the energy of UV irradiation to the line region increased. As the UV irradiation energy increases, the number of radical species initiated from the photoinitiator increases, and more chain extension reactions and crosslinking reactions proceed. An increase in storage modulus confirms the increase of the crosslinking density. As shown in Fig. 2a, it was observed that the Young's modulus of the line region of each pattern increases with increasing UV energy irradiation and increasing pattern number. In contrast, each pattern's modulus of the isolated region decreased with increasing UV energy irradiation and pattern number, as shown in Fig. 2b. The isolated and line regions of each pattern were appositely and separately cured according to the irradiated UV energy of each region.

3.2. Storage modulus

The storage modulus value of the whole PSA sample containing both high and low cured region does not show a very large difference between samples, but shows a clear trend: the storage modulus of each patterned sample (Fig. 3) tended to increase with increasing curing density in one region. Dividing the PSA into two same-sized regions while irradiating them at different UV energies using a photomask results in a higher curing density in one region over the other. Despite the

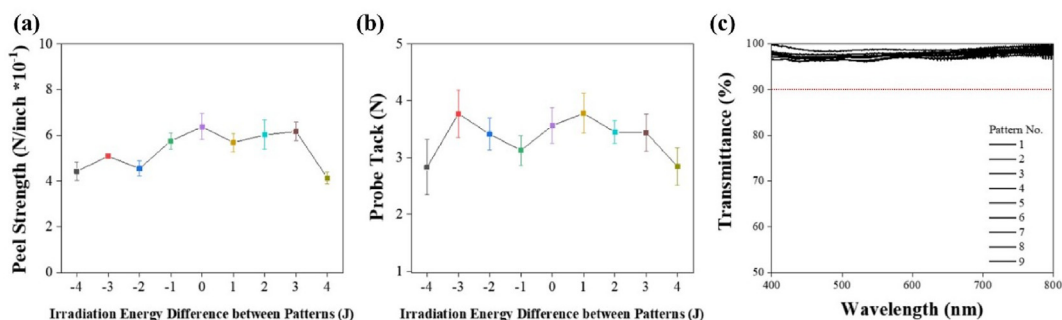


Fig. 5 – (a) Peel strength, (b) Probe tack, and (c) Transmittance property of the UV pattern cured PSA samples. There is a guide-line at the 90% transmittance.

differences in curing densities, the entire sample's storage modulus tends to depend on regions with high curing density (Fig. 3). Conversely, patterns 1 and 9 exhibited a decrease in the storage modulus of the entire sample. Both samples were cured under extreme conditions (energy of 0 J in one area and 4 J in the other, Fig. 1a), which resulted in the incomplete curing of one region, i.e., the difference in the curing densities between the regions was extremely large. The non-patterned sample (pattern 5) exhibited a storage modulus value of 12.8 kPa, while those of pattern 1 and 9 are 16.1 and 11.7 kPa, respectively. It is difficult to explain the similar physical properties of patterns 1, 5, and 9, as indicated by their storage moduli, despite their different curing densities. The more even storage modulus was observed in patterns 6–9. Here, the PSA curing pattern was divided into a line and grid area, and the line area had a relatively high curing density. In contrast, when the isolated region had a high curing density (patterns 1–4), a relatively high variability in the storage modulus value was measured. The line regions are physically connected, which explain the stable physical properties of the sample.

3.3. Flexibility: strain recovery and stress relaxation properties

The difference in the roles of the line and island areas, as determined by the different storage moduli of the sample, was also seen in the varying stress recovery properties. The patterned samples (6–8), which showed a high modulus due to the high curing density in the connected line region also showed better recovery performance than the non-patterned sample (pattern 5). For the sample with a highly cured connected region, the trend of the strain recovery properties followed that of the storage modulus. An increase in the storage modulus of the sample yielded excellent recovery properties (patterns 6–8) (Fig. 4c, R^2 is 0.9) because the physically connected line area provides structural stability. This is the same result as reported in previous paper [19]. The modulus and recovery performance are determined by the interaction of molecules in each region cured non-homogeneously with different curing densities. The interconnected high-cured line region acts like a rope that provides strong support throughout the sample. Furthermore, the stress applied to the sample was unequally distributed throughout the sample, but was concentrated at both points of the sample because of the bending modulus. However, the high-modulus line region is

linked through the whole sample, which enables the dispersion of the concentrated stress at both ends along the line region. In addition, owing to the difference in the curing density, it was expected that the samples will exhibit a synergistic effect by flexibly stretching the lower cured area and buffering the plastic deformation of the highly cured area when under strain. In contrast, in patterns 1–4, which consisted of the highly cured isolated region and low cured line region, the isolated region at both ends endured all of the concentrated stress on its own, resulting in interfacial and cohesive failure of the PSA. Therefore, no significant correlation was observed between the modulus and recovery performance of pattern 1–5 samples (Fig. 4d). Furthermore, the strain recovery value decreased as the difference in the curing density became larger (patterns 1 and 9), which was in agreement with the storage modulus trend.

The stress relaxation property was almost constant for moderate curing conditions (patterns 2–8), whereas it fluctuated under extremely large differences in curing densities, i.e., it sharply increased for pattern 1, and sharply decreased for pattern 9. Pattern 1 is characteristic of an extremely low crosslinking density of the line region and a high viscosity. Therefore, there was no strong resistant force at the crosslinking site when the sample was stretched, i.e., it stretched easily. Consequently, the polymer chains of the PSA easily moved, and the applied stress was well-dispersed resulting in good stress relaxation properties, and low recovery performance because it nearly has the elastic force. In case of pattern 9, the line region was highly cross-linked and cured, which resisted the stretching of the sample resulting in an inferior stress relaxation performance. In addition, the isolated region barely exhibits a recovery performance because of its extremely low crosslinking density. Thus, it can be concluded that because the strain recovery performance depends only on the line region without synergistic effect or both region, pattern 9 exhibits a lower recovery performance than other patterned samples (6–8).

3.4. Applicability to OCA: adhesion properties and transmittance

The probe tack and peel strength data are shown in Fig. 5. The patterns 1–4 and 6–9 samples showed similar adhesive properties than the non-patterned sample (pattern 5). Regarding peel strength, the non-patterned sample showed

the highest value of 0.63 N/in. On the contrary, the patterned samples showed a tendency to slightly decrease, but maintained a similar adhesive performance (0.41–0.61 N/in) without significant deterioration (Fig. 5a). Regarding probe tack, with the exception of the pattern 1 and 9 samples with the extreme curing energy difference, most of the samples (pattern 2–8) maintained similar adhesive properties between 3.1 and 3.7 N (Fig. 5 (b)).

The representative data (pattern 8) of the measured transmittance are shown in Fig. 5. All samples showed similar transparency values of above 90% compared to the empty air reference. Thus, the patterned samples were transparent enough for application in an optically clear display adhesive.

4. Summary and conclusions

We determined the effect of the different patterns of ultraviolet (UV) curing crosslinking density on the flexibility properties of optically clear acrylic PSAs. After confirming the formation of the UV curing pattern in the pressure-sensitive adhesives (PSAs), the strain recovery and stress relaxation performance were measured to check their applicability in flexible displays. Compared to the non-patterned sample, the patterned sample showed a significant improvement in the recovery performance when the difference in UV curing energy between the patterns was 2–3 J. The patterned sample exhibited a relatively high modulus compared to the non-patterned sample, when the energy difference was 2–3 J between the patterns. Finally, the adhesive performance of the PSA was maintained except for the sample with the largest energy difference (4 J). Furthermore, all samples showed excellent transparency and applicability to optically clear adhesives (OCAs). In conclusion, our results show that implementing the curing density patterning technology during the UV irradiation process can maintain the adhesive properties and transparency, while improving recovery properties of the PSAs without changing the pre-polymer resin composition or additive content. However, the adhesion performance of patterned samples did not decrease compared to the non-pattern sample, but there is a limit that the adhesion performance does not fit the degree required for actual applications. This can be supplemented by adjusting the blending ratio of the adhesive resin and the content of additives, such as a crosslinking agent and photoinitiator. Therefore, it is necessary to conduct a related performance optimisation study later.

Impact statement

PSA UV pattern curing expands the scope of its research for flexible displays and paves the way for new directions in enabling human understanding and use of cutting-edge technologies.

Data availability

The raw/processed data required to reproduce these findings cannot be shared at this time as the data also forms part of an ongoing study.

Declaration of Competing Interest

The authors declare that they have no known competing financial interests or personal relationships that could have appeared to influence the work reported in this paper.

Acknowledgments

This work was financially supported by the Samsung Display Co., Ltd.. We would like to thank Anton Paar Korea and Seol-Hee Jeon of Anton Paar Korea for their support with the rheological tests.

REFERENCES

- [1] Koo IM, Jung K, Koo JC, Nam J, Lee YK, Choi HR. Development of soft-actuator-based wearable tactile display. *IEEE Trans Robot* 2008;24(3):549–58.
- [2] Jung S, Kim JH, Kim J, Choi S, Lee J, Park I, et al. Reverse-micelle-induced porous pressure-sensitive rubber for wearable human–machine interfaces. *Adv Mater* 2014;26(28):4825–30.
- [3] Zhou L, Wanga A, Wu S-C, Sun J, Park S, Jackson T. All-organic active matrix flexible display. *Appl Phys Lett* 2006;88(8):083502.
- [4] Geffroy B, Le Roy P, Prat C. Organic light-emitting diode (OLED) technology: materials, devices and display technologies. *Polym Int* 2006;55(6):572–82.
- [5] Park J-S, Kim T-W, Stryakhilev D, Lee J-S, An S-G, Pyo Y-S, et al. Flexible full color organic light-emitting diode display on polyimide plastic substrate driven by amorphous indium gallium zinc oxide thin-film transistors. *Appl Phys Lett* 2009;95(1):013503.
- [6] Li G, Wang W, Yang W, Lin Y, Wang H, Lin Z, et al. GaN-based light-emitting diodes on various substrates: a critical review. *Rep Prog Phys* 2016;79(5):056501.
- [7] Colley A, Pflöging B, Alt F, Häkkinen J. Exploring public wearable display of wellness tracker data. *Int J Hum Comput Stud* 2020;138:102408.
- [8] Kim J, Shim HJ, Yang J, Choi MK, Kim DC, Kim J, et al. Ultrathin quantum dot display integrated with wearable electronics. *Adv Mater* 2017;29(38):1700217.
- [9] 23rd international conference on intelligent user interfaces. In: Luzhnica G, Veas E, editors. Investigating interactions for text recognition using a vibrotactile wearable display; 2018.
- [10] Lee J-G, Shim G-S, Park J-W, Kim H-J, Han K-Y. Kinetic and mechanical properties of dual curable adhesives for display bonding process. *Int J Adhes Adhes* 2016;70:249–59.
- [11] Lee J-H, Lee T-H, Shim K-S, Park J-W, Kim H-J, Kim Y, et al. Effect of crosslinking density on adhesion performance and flexibility

- properties of acrylic pressure sensitive adhesives for flexible display applications. *Int J Adhes Adhes* 2017;74:137–43.
- [12] Park C-H, Lee S-J, Lee T-H, Kim H-J. Characterization of an acrylic polymer under hygrothermal aging as an optically clear adhesive for touch screen panels. *Int J Adhes Adhes* 2015;63:137–44.
- [13] Benedek I, Feldstein MM. *Handbook of pressure-sensitive adhesives and products*: three volume set. CRC Press; 2019.
- [14] Creton C. *Pressure-sensitive adhesives: an introductory course*. *MRS Bull* 2003;28(6):434–9.
- [15] Mapari S, Mestry S, Mhaske S. *Developments in pressure-sensitive adhesives: a review*. *Polym Bull* 2020:1–34.
- [16] Benedek I. *Pressure-sensitive formulation*. CRC Press; 2020.
- [17] Barisa RE, Resalati H, Monfared MHA, Ghasemiyan A, Shakeri A. In: *The structure and physical -chemical properties of polymers in pressure-sensitive adhesives (PSA)*. Polymerization; 2014.
- [18] Class JB, Chu S, editors. *The viscoelastic properties of pressure-sensitive adhesives*; 1984.
- [19] Back J-H, Baek D, Sim K-B, Oh G-Y, Jang S-W, Kim H-J, et al. Optimization of recovery and relaxation of acrylic pressure-sensitive adhesives by using UV patterning for flexible displays. *Ind Eng Chem Res* 2019;58(10):4331–40.
- [20] Lee JH, Myung MH, Baek MJ, Kim H-S, Lee DW. Effects of monomer functionality on physical properties of 2-ethylhexyl acrylate based stretchable pressure sensitive adhesives. *Polym Test* 2019;76:305–11.
- [21] Joo H-S, Park Y-J, Do H-S, Kim H-J, Song S-Y, Choi K-Y. The curing performance of UV-curable semi-interpenetrating polymer network structured acrylic pressure-sensitive adhesives. *J Adhes Sci Technol* 2007;21(7):575–88.
- [22] Back J-H, Baek D, Park J-W, Kim H-J, Jang J-Y, Lee S-J. Shock absorption of semi-interpenetrating network acrylic pressure-sensitive adhesive for mobile display impact resistance. *Int J Adhes Adhes* 2020;99.
- [23] Oliver WC, Pharr GM. An improved technique for determining hardness and elastic modulus using load and displacement sensing indentation experiments. *J Mater Res* 1992;7(6):1564–83.
- [24] Pharr G, Oliver W. Measurement of thin film mechanical properties using nanoindentation. *Mrs Bull* 1992;17(7):28–33.